

AlloyASG: Alloy Predicate Code Representation as a Compact Structurally Balanced Graph

Guanxuan Wu

Allison Sullivan

gxw6804@mavs.uta.edu

allison.sullivan@uta.edu

University of Texas at Arlington

Arlington, Texas, USA

ABSTRACT

In the program analysis and automated bug-fixing fields, it is common to create an abstract interpretation of a program’s source code as an Abstract Syntax Tree (AST), which enables programs written in a high-level language to have various static and dynamic analyses applied. However, ASTs suffer from exponential growth in their data size due to the limitation that ASTs will often have identical nodes separately listed in the tree. To address this issue, we introduce a novel code representation schema, Complex Structurally Balanced Abstract Semantic Graph (CSBASG), which represents code as a complex-weighted directed graph that lists a semantic element as a node in the graph and ensures its structural balance for almost finitely enumerable code segments, such as the modeling language Alloy. Our experiment ensures that CSBASG provides a one-on-one correspondence of Alloy predicates to complex-weighted graphs. We evaluate the effectiveness and efficiency of our CSBASG representation for Alloy models and identify future applications of CSBASG for Alloy code generation and automated repair.

KEYWORDS

Alloy, Abstract Semantic Graphs, Program Representation, Automatic fixing, Structural balance, Complex-weighted graphs

1 INTRODUCTION

Alloy [16] is a declarative, relational logic-based modeling language for describing structural and dynamic properties of a system’s design. Since Alloy is used to verify software system designs [40, 5, 34, 8], and to perform various forms of analyses over the corresponding implementation, including deep static checking [17, 10], systematic testing [22], data structure repair [39], automated debugging [12] and to synthesize security attacks [2, 23, 29], the consequences could be catastrophic if an Alloy model is faulty yet successfully compiles. Several iterative search methods based on ASTs have already been implemented for automated repair and partial generation of Alloy models [32, 14, 42, 7]. However, any iterative search methods for mutants or AST elemental changes that fix the Alloy code segments require expansive storage and have intractable search spaces due to the exponential growth of the code segment length, limiting their computational efficiencies.

In recent years, there have been several bodies of work that focus on automatically repairing programming code using machine learning techniques [30, 20, 13, 3, 38, 15, 28]. Such works provide valuable inspiration to us since we have a dataset of real-world fixing pairs consisting of faulty predicates written by the students

and their correct counterparts [21], effectively leading to a set of pairs of inputs and ground truths. Nonetheless, almost all the sequence-based algorithms treat the code segments as natural language sequences with a black-box function trained for faulty code as input and corrected code as output. These approaches ignore the strict logic of the programming languages, severely hindering the explainability of the process.

To create a machine learning algorithm that is aware of the logic of the programming language we are generating code in, we need a logical structure-aware, vectorized, machine-and-human-readable, and computationally efficient code representation that improves upon the AST adjacency matrix representation that grows exponentially in size. Some of the representation learning methods [4, 25] train functions that output vectors from the AST, yet the nature of their dependency on the control flow paths in the AST of those general-purpose languages renders their methodologies implausible for a specification language such as Alloy, which is declarative and lacks control flow. Other methods [41, 33, 35] try to focus on the raw AST for a universal representation, yet those algorithms still suffer from rapid growth in the size of the AST. Therefore, this paper aims to create a structure that generates a compact representation of the code segment, yet still gives the same complete information as the raw AST. Recent work created an Abstract Semantic Graph (ASG) [9], which is close to meeting our data representation needs, but the original designation lacks a numerical representation that provides an adjacency or Laplacian matrix that could be used in popular graph machine learning algorithms [24, 11, 18, 31, 27]. Therefore, in this paper, we introduce a matrix representation of the ASG with the following objectives:

- (1) one-on-one correspondence between the source code, the AST, and the graph matrix;
- (2) better performance in compactness and possible space-saving than the raw AST representation;
- (3) allowing a direct comparison of the difference between the pair of code segments before and after manual fixing.

Such goals could be impractical for general-purpose, high-level languages such as C or Java, as most languages have a complicated type system and data structures that are not finite or even integer-enumerable. Despite that, for a simple, declarative, almost finitely enumerable language such as Alloy, we could create a Complex-weighted Structurally Balanced Abstract Semantic Graph (CSBASG) that translates the code segments into compact graphs for the subset covering most of the possible combinations.

One of the advantages of the graph is the uniqueness of the semantics. For two semantically different terms in an AST, e.g.,

a variable or a unary or binary operator, there will only be one corresponding vertex in the CSBASG. This intuitively represents the code elements and their relationships with a reduced space cost. Besides, for a fixing pair of code segments consisting of the faulty code and its correction, CSBASG could align the modifications by the common node signatures shared by the pair and compare their structural differences.

Therefore, in this paper, we make the following contributions:

CSBASG: We introduce the concept of a CSBASG that meets our three objects (one-to-one correspondence, more compact, and supports direct comparisons). We provide an algorithm to convert an AST into a CSBASG and convert a CSBASG back to an AST and corresponding code segments.

Application to Alloy: We tailor the generation of CSBASG to the Alloy modeling language.

Evaluation: We evaluate the improvement on compactness and density of a CSBASG compared to an AST and evaluate how to compare multiple CSBASGs.

Open Source: We release our source code to produce <https://github.com/AlexandervonWu/AlloyASG-Release>.

2 BACKGROUND

In this section, we describe key components of Abstract Semantic Graphs and the Alloy modeling language.

2.1 Abstract Syntax Tree and Abstract Semantic Graph

We use the common notation of the abstract syntax tree (AST) for the raw representation of the syntactic structure of the Alloy source code [6]. We follow the formal definitions from [19]:

DEFINITION 1 (CONTEXT-FREE GRAMMAR). [19] *A context-free grammar (CFG) $G \equiv (N, \Sigma, R, s)$ is a tuple where N is the set of nonterminals, Σ is the set of terminals, R is the set of production rules $a \rightarrow b_1 b_2 \dots b_N$ where $a \in N$ is a nonterminal and $b_i \in N \cup \Sigma$, and $s \in N$ is the starting nonterminal of the grammar. The language of G is the set of strings from the starting non-terminal.*

DEFINITION 2 (AST). [19] *Given a context-free grammar (CFG) $G = (N, \Sigma, R, s)$, an abstract syntax tree (AST) $T \equiv (G, X, r, \xi, \sigma)$ is a tree with a set of nodes X , a root node $r \in X$, a mapping $\xi : X \rightarrow \mathcal{P}(X)$ from each of the nodes to a subset of nodes as its children and each child set $\forall x \in X : \xi(x)$ is either empty or well-ordered, and $\sigma : X \rightarrow (N \cup \Sigma)$ maps each node to its corresponding label as a terminal or nonterminal word in the CFG.*

According to [9], an abstract semantic graph (ASG) resolves the branches defining the properties of a node in the AST to its original definitions. But here, to create a more compact form of ASG specifically for Alloy, we use a more radical definition that combines every syntactically and semantically equivalent node as below:

DEFINITION 3 (ASG). *Given a CFG $G = (N, \Sigma, R, s)$, an abstract semantic graph (ASG) $\mathcal{G} \equiv (G, \mathcal{V}, \mathcal{E}, r)$ where $\mathcal{V} \subseteq N \cup \Sigma$ is a set of nonterminal and terminal words as nodes (vertices) of the graph, and $\mathcal{E} \subseteq \mathcal{V} \times \mathcal{V} \times \mathbb{C}$ is the set of edges between the words with the edge weight between nodes $v_i, v_j \in \mathcal{V}$ be $w_{ij} \in \mathbb{C}$, and r is the root of the corresponding AST of the ASG, i.e. the first node being visited.*

Note that since \mathcal{E} is an arbitrary set of edges in forms of (v_i, v_j, w_{ij}) , an AST or empirical construction of ASG could have more than one set of $\{w_{ij}\}$ to represent. If the weight function $w : \mathcal{V} \times \mathcal{V} \rightarrow \mathbb{C}$ ensures that $w_{ij} \neq 0$ if and only if there exists an edge from v_i to v_j , and $w_{ij} \neq w_{ik}$ for any $j \neq k$ be children of i , either at the same order of execution (children under the same node in the corresponding AST) or at the different order (if a nonterminal presents more than once in the AST and each time comes with a set of children). There could also be multiple AST links connecting two ASG nodes, and we will discuss how we form a weight value for this case in Section 3.

2.2 Complex-weighted Graph and its Structural Balance

Since Definition 3 gives a complex-weighted graph and our requirement for a vectorization of such ASG, the construction of the graph requires the edge values specifying the relationships between any of the two nodes. So we borrow the structural balance concept from [36]:

DEFINITION 4 (COMPLEX-WEIGHTED STRUCTURAL BALANCED GRAPH). [36] *For a graph $\mathcal{G} = (\mathcal{V}, \mathcal{E})$, let $a_{ij} = w_{ji}$ be the entries of the adjacency matrix A where $|a_{ij}| > 0$ indicates there exists an edge between v_j and v_i , then the graph \mathcal{G} is said to be structurally balanced if all the entries of its adjacency matrix $A = [a_{ij}]^{N \times N}$ satisfies $a_{ij} \equiv |a_{ij}| \angle \theta_{ij} = |a_{ij}| \angle (\theta_i - \theta_j)$, where $\theta_1, \dots, \theta_N \in (-\pi, \pi)$ is called the signatures of the nodes $v_1 \dots v_N$, respectively.*

In the ASG context, intuitively, the signatures of the nodes $\theta_1, \dots, \theta_n$ could encode the syntactic and semantic properties of each terminal or nonterminal node and the magnitudes of each edge $|a_{ij}|_{i,j \in \{1 \dots N\}}$ encodes their relative properties, such as if a node is the left (1st) or right (2nd) child of a binary operator. We chose this concept for its mathematical solid properties. Let $d_i = \sum_{j \in 1}^N |a_{ij}|$ which is the in-degree of node v_i and let $D = \text{diag}(d_1, \dots, d_N)$ be the diagonal matrix giving the in-degrees of each node on their corresponding rows, and define $L = D - A$ as the Laplacian matrix, then we have the lemma below [36]:

LEMMA 1. [36, 37]

The following are equivalent:

- (1) *Complex weighted graph $\mathcal{G}(A)$ is structurally balanced.*
- (2) *Zero is a eigenvalue of L with eigenvector $\zeta = [1 \angle \theta_1, \dots, 1 \angle \theta_N]^T$.*
- (3) *$D_\zeta := \text{diag}(\zeta)$ such that $\hat{A} = D_\zeta^{-1} A D_\zeta$ is nonnegative and $\hat{A} = [|a_{ij}|]_{N \times N}$.*
- (4) *$D_\zeta := \text{diag}(\zeta)$ such that $\hat{L} = D_\zeta^{-1} L D_\zeta$ has a zero eigenvalue with an eigenvector being $\mathbf{1}$, where $\hat{L} = D - \hat{A}$.*

PROOF. See proof of Lemma 1 in [37]. □

Notably, in the notation of [36, 37], each column specifies the outer edges of a node, and the row-based adjacency matrix must be transposed before acquiring the Laplacian.

2.3 Alloy

Alloy users write models that describe the properties of the system of interest. Then, the Analyzer helps the user understand their

<pre style="margin: 0;"> (a) 1. sig Person { 2. Tutors : set Person, 3. Teaches : set Class 4. } 5. sig Group 6. sig Class { Groups : Person -> Group } 7. sig Teacher in Person {} 8. sig Student in Person {} </pre>	<pre style="margin: 0;"> (b) /* Assuming a universe of 3 persons, the tutoring * chain of every person eventually reaches a Teacher. */ 9. pred inv15oracle { 10. all p:Person some Teacher&(^Tutors).p 11. } </pre>	<pre style="margin: 0;"> (c) 12. pred inv15 { 13. all p : Person { some t : Teacher { 14. t in p.Tutors 15. or t in p.Tutors.Tutors 16. or t in p.Tutors.Tutors.Tutors 17. }} 18.} </pre>
---	--	--

Figure 1: Alloy Model of a Classroom Management System with an oracle and student submission for inv15

system by displaying the consequences of their properties, helping identify any missing or incorrect properties, and exploring the impact of modifications to those properties. To achieve this, the Analyzer uses off-the-shelf SAT solvers to search for scenarios, which are assignments to the sets and relations of the model such that all executed formulas hold. These scenarios are presented visually and introduce a separation of concern between writing and exploring a specification. If no such scenario can be found, the Analyzer reports that the formulas are unsatisfiable.

To highlight how modeling in Alloy works, Figure 1 depicts the base model of a classroom management system. This model is from the Alloy4Fun dataset, which is a collection of submissions made by novice users learning Alloy [21]. Signature paragraphs introduce named sets and can define relations, which outline relationships between elements of sets. Line 1 introduces a named set `Person` and establishes that each `Person` atom connects to any number of (set) `Person` atoms through the `Tutor` relation and each `Person` atom connects to any number of (set) `Class` atoms through the `Teaches` relation. Line 5 introduces the named set `Group`, which contains no relations. Line 6 introduces the named set `Class` and states that each class has a set of people assigned to a group using the ternary relational `Groups`. Lines 7 and 8 introduce the named sets `Teacher` and `Student` as subsets (in) of `Person`.

Predicate paragraphs introduce named first-order, linear temporal logic formulas that can be invoked elsewhere. Figure 1 (b) depicts the oracle for exercise `inv15`. The predicate `inv15oracle` uses universal quantification (‘all’), set multiplicity (‘some’), set intersection (‘&’), transitive closure (‘^’), and relational join (‘.’) to express that for every person, there is an intersection between the set `Teacher` and the set of `Tutors` reachable by one or more invocation of `Tutor`’s relation. The student submission in Figure 1 (c) is faulty, and is overconstrained, which means the faulty formula prevents instances that should have been generated, and underconstrained, which means the faulty formula allows both instances that should have been prevented. The student attempted to use nested quantification to explicitly outline that a teacher should be reachable in 1 to 3 traversals down the `Tutor`’s relation.

2.4 Alloy Grammar

We consider the Alloy grammar [16] before constructing the graph representation. The basic blocks under the overall root of an Alloy model, `ModelUnit`, consists of a set of declarations, such as signatures as basic types, functions as processes, and predicates as logical arguments. Our dataset Alloy4Fun [21] covers only simple predicates without references to external libraries; therefore, creating representations for those code segments included in the

dataset is an ideal starting point. Figure 2 gives an example of an Alloy predicate in the dataset that contains 32 AST nodes. From this representation, it is obvious that the raw AST representation has been relatively huge and complicated, even with a short segment of code enveloped in a single predicate, mostly due to the redundancy of the semantically identical nodes presenting in the AST for their multiple appearances in the original code. In the given example, there are three binary operators “in”, and 6 dots (JOIN) as operators; these would all be treated as distinct nodes in a raw AST representation.

A predicate defines a scope that contains an expression while itself is a solid, invariant root for any fixing pairs. We can easily enumerate all possible nodes under an expression (or formula): the finitely enumerable types of expressions or formulae, plus variable declarations that only occur under the quantifiers of first-order logic. In this paper, we assign them fixed signatures, yet an adaptive signature system could be used in case of an extension of the CSBASG into either more types of nodes or extra optimizations.

Another property of Alloy is that almost all expression or formula nodes have a finite and fixed number of children, for instance, 1 for unary operators, 2 for binary operators, and 3 for the if-then-else sentences. In these cases, there could be a trivial, polynomial-based implementation of the $|w_{ij}|$ values for the edges between such a node v_i and one of its children v_j . Even so, there are some exceptions, such as a function call (having an indefinite number of parameters), a list expression or formula (for example, the consecutive logical ANDs and ORs for a conjunctive or disjunctive normal form), or a set of variable declarations for the same quantifier. We will handle them on a case-by-case basis in Section III.

3 CSBASG CONSTRUCTION

Intuitively, to create an ASG following *Definition 3*, we first need to do a pre-order traversal on the AST to identify and combine the semantically identical nodes. We start by constructing an isomorphism between \mathcal{V} and $N \cup \Sigma$, then rewrite each AST link into an ASG edge. The isomorphism is trivial since AST nodes with the same word are combined into the same node in the ASG. Nonetheless, constructing the ASG edge set by the AST relations ξ requires a cautious step: merging two AST nodes requires clarifying the orders of the visit to avoid confusion. or instance, in the example given in Figure 1, if we consider the binary operator “IN” as a single node without specifying the order of execution, we would not specify which could be put at the right of the operator, “p.Tutors”, “p.Tutors.Tutors” or “p.Tutors.Tutors.Tutors”. A naive approach that deviates a bit from the ASG definition is to use two numbers for the weight values w_{ij} instead of one, that is, for any of the existing

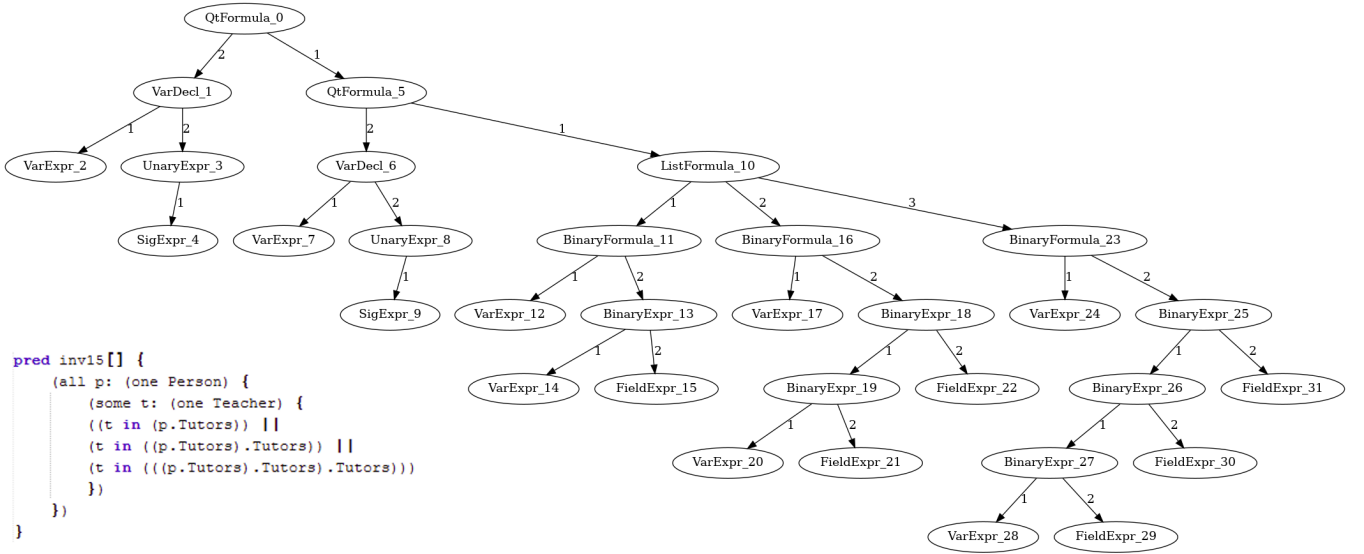


Figure 2: An instance of an Alloy predicate in the dataset parsed with pretty string and its raw AST representation.

link $x_2 \in \xi(x_1)$ in the AST, defining $v_1 = \sigma(x_1), v_2 = \sigma(x_2)$. Then, we create an edge between v_1, v_2 with a weight-pair $(\omega, t) \in \mathbb{N} \times \mathbb{N}$, specifying that x_2 is the ω -th child of x_1 in the order defined for $\xi(x_1)$, and it is the t -th time to visit v_1 in the program logic.

Nevertheless, we expect that with a matrix form of ASG, we could take advantage of their linearity, especially for the potential application of machine learning operations. In addition, a matrix form of the graphs could be more easily compared with respect to multiple implementations of a predicate or other code segments of interest. With the naive construction above, it is challenging to proceed since the mapping from the pair given above to the edge value that serves as an entry in the adjacency matrix is nontrivial. Here, we could define $\mathcal{M} : \mathbb{N} \times \mathbb{N} \rightarrow \mathbb{R}$ as mapping such that $\mathcal{M}(\omega, k)$ gives the entry in the matrix form of an ASG if it is the sole AST link in the ASG. The mapping could be defined arbitrarily, provided that it maintains injectivity to avoid the simple, different-edge-same-value confusion (we will call it Type 1 Confusion later). Such forms the real part (magnitude) of the edges in the CSBASG.

Considering all the above, we formally define the complex-valued structurally balanced ASG as a subset of the general ASG constructions that maintain the structural balance.

DEFINITION 5 (COMPLEX-VALUED STRUCTURALLY BALANCED ASG (CSBASG)). A Complex-valued Structurally Balanced ASG is a type of ASG $\mathcal{G} \equiv (G, \mathcal{V}, \mathcal{E}, r)$ where there exists a vector $\{\theta_1, \theta_2, \dots, \theta_{|\mathcal{V}|}\}$, such that the weights in each of the edge $(v_i, v_j, w_{ij}) \in \mathcal{E}$ satisfy $w_{ij} = |w_{ij}| \angle (\theta_i - \theta_j)$. For each of the node $v_i \in \mathcal{V}$, $\theta_i \in (-\pi, \pi)$ is called the signature of v_i .

Algorithm 1 is a high-level process to convert an AST to a CSBASG. It follows the process of an abstract interpretation, where \vec{t} in the recursive part gives a simplified interpretation state tracking the times of node visitations in the pre-order traversal of the AST. We initialize the nodemap and the list of angular signatures for each node, with the only element being the dummy overall root, and

assign each node an angular signature with regard to the predefined assignment, outlining every unique signature; the number of unique angular signatures (semantically distinct nodes) is the number of rows and columns of the resulting adjacency matrix. After that, we initialize a state vector \vec{t} to count the times of the order of the visit to each node. A recursive function will then iterate over the AST beginning from the overall root, update the adjacency matrix for each downlink from the root node according to the composition function β and the encoding method \mathcal{M} , while updating the counter of the given node with the corresponding entry of the state vector signaling the pre-order time of identical appearance in the AST before recursively visit the subtree with the new root being a child of the local root.

In general, with a static signature assignment φ , the algorithm terminates in $O(|X|)$ since each of the nodes in the AST was visited exactly once and $|\mathcal{V}| < |X|$ strictly. We say an ASG is *generated* by an AST if the AST was converted to the same ASG with the same signature assignment and magnitude mapping.

By Definition 5, for a given Alloy predicate as an input, define a fixed unique root $r \equiv v_1$, which is the predicate itself, and such root node is unique in each predicate. We can intuitively assign $\theta_1 = \varphi(\sigma(r)) \equiv 0$ as a starting point. Besides, we expect the same input parameters for the pairs of predicates to be directly compared, so the overall root node of each predicate only has one child, the local root expression or formula. Therefore, the only work left is to define the signature assignment function φ on the subset that could present under a tree rooted by an expression or formula.

Another notable function, \mathcal{M} , could be defined in multiple ways if it maintains a one-on-one correspondence between the syntactic positions and the execution or tree-walking order. However, for an AST with multiple syntactically and semantically identical nodes, multiple edges connect them, but they could have different positions ω and thus different \mathcal{M} values. So, given an AST, we can define the three types of confusion that could happen in an ASG construction:

Algorithm 1 Convert AST to CSBASG

```

1: Input: an AST  $T \equiv (G, X, r, \xi, \sigma)$  parsed from the original code
   of an Alloy predicate, with root node  $r$ ; an injective function
    $\varphi : N \cup \Sigma \rightarrow (-\pi, \pi)$  to map the words to their unique signature,
   and another injective function  $\mathcal{M} : \mathbb{N} \times \mathbb{N} \rightarrow \mathbb{R}$  outputs the
   magnitude of an AST edge given the positional argument of
   a link and the time has the sourcing node been visited. For
   the entries, we use  $\beta$  as a recursive encoder that calculates the
   matrix entries iteratively.
2: Output: a CSBASG  $\mathcal{G}(A)$  representing  $T$  with its adjacency
   matrix  $A$ , and the signatures of the nodes  $\{\theta_0, \theta_1, \theta_2, \dots, \theta_{|\mathcal{V}|}\}$ ,
   each corresponds to a column of  $A$ .
3:  $\vec{\theta} \leftarrow [0]$ 
4:  $\text{nodemap} \leftarrow [(r, 0)]$ 
5:  $\mathcal{V} \leftarrow \{r\}$ 
6: for  $i \leftarrow 2, \dots, |X|$  do
7:    $\text{node} \leftarrow X_i$ 
8:    $\theta_i \leftarrow \varphi(\sigma(\text{node}))$ 
9:   if  $\theta_i \notin \vec{\theta}$  then
10:     $\vec{\theta} \leftarrow \vec{\theta} :: \theta_i$ 
11:     $\mathcal{V} \leftarrow \mathcal{V} :: \text{node}$ 
12:   end if
13:    $\text{nodemap} \leftarrow \text{nodemap} :: (\text{node}, \theta_i)$ 
14: end for
15:  $A_0 \leftarrow [0]_{|\mathcal{V}| \times |\mathcal{V}|}$ 
16:  $A \leftarrow \text{ENCODE-RECURSIVE}(r, \vec{\theta}_{|\mathcal{V}|}, A_0)$ 
17: return  $A, \vec{\theta}$ 
18: function ENCODE-RECURSIVE( $r_t, \vec{t}, A_{\vec{t}}$ )
19:    $\theta_t \leftarrow \text{nodemap.GET}(r_t)$ 
20:    $i \leftarrow \vec{\theta}.\text{GET-INDEX}(\theta_t)$ 
21:    $t \leftarrow \vec{t}.\text{GET}(i)$ 
22:    $\vec{t}' \leftarrow \vec{t}$ 
23:    $\vec{t}'[i] \leftarrow t + 1$ 
24:    $A_{\vec{t}'} \leftarrow A_{\vec{t}}$ 
25:   for  $\omega \leftarrow 1, \dots, |\xi(r_t)|$  do
26:      $c \leftarrow \xi(r_t).\text{GET}(\omega)$ 
27:      $\theta_c \leftarrow \text{nodemap.GET}(c)$ 
28:      $j \leftarrow \vec{\theta}.\text{GET-INDEX}(\theta_c)$ 
29:      $A_{\vec{t}'}[j, i] \leftarrow \beta(\mathcal{M}(\omega, t), A_{\vec{t}}[j, i]) \cdot \angle(\theta_i - \theta_j)$ 
30:      $A_{\vec{t}'} \leftarrow \text{ENCODE-RECURSIVE}(c, \vec{t}', A_{\vec{t}'})$ 
31:   end for
32:   return  $A_{\vec{t}'}$ 
33: end function

```

DEFINITION 6 (COMPLETENESS OF CSBASG). Given a class of AST $T \equiv (G, X, r, \xi, \sigma)$, we say a CSBASG construction is **complete** if the parser L outputs the AST correctly by the generated CSBASG in Algorithm 1; that is, none of the confusions formed in the construction of \mathcal{M} and β mappings:

- If \mathcal{M} is not injective, i.e., for two edges with positional values $\omega_1 \neq \omega_2$ or tree-walking orders $t_1 \neq t_2$, $\mathcal{M}(\omega_1, t_1) = \mathcal{M}(\omega_2, t_2)$. This situation is a Type 1 Confusion, or Incomplete Edge Mapping Confusion.

- If an ASG parser L cannot parse a multi-edge in an ASG that corresponds to two AST links that have the same parent and different but syntactically and semantically equal children with different positions, e.g., $(a+b) - (c+d)$ where the central binary operator $-$ has two syntactically and semantically equal children of binary operator nodes $+$, then the situation causes a Type 2 Confusion or Twin Children Confusion.
- If an ASG parser L cannot parse a multi-edge in an ASG that corresponds to two AST links connecting semantically and syntactically equivalent pairs of nodes, but the parent nodes are at different positions in the AST, e.g., $(a \wedge b) \vee (a \wedge c)$, the ASG node “ \wedge ” has two left children of terminal node a , then the situation causes a Type 3 Confusion or Twin Parent Confusion.

Here, the goal becomes creating the mappings \mathcal{M} and β that ensure the parser L is free of confusion.

Polynomial-based Static CSBASG Encoding

By Definition 6, intuitively, the signature assignment φ is not relevant to the completeness of a CSBASG; that function could be arbitrarily defined or even *learned*. However, the processes directly related to the fidelity of the representation scheme must be re-defined to ensure the completeness of the CSBASG. A naive implementation could consider the ω positional values as sequential numbers 1, 2, ... and add them together for the representation; however, if there is a ternary operator tor , then $\text{tor}(a, a, c)$ will have its children-position map be defined as $\{a : 3, c : 3\}$, causes confusion that has two children with a position 3 (and therefore, missing positions 1 and 2), causes a Type 2 confusion.

Here, we introduce the polynomial-based, integer-magnitude static CSBASG encoding for a theoretical language: each AST generated from its CFG has a maximum number of children p . Then, let T be the maximum number of syntactic and semantically identical nodes in the code segment. For the AST link drawn from a node to its $(\omega + 1)$ -th child, let $\mathcal{M}(\omega, t) = 2^{(t-1)p+\omega}$ and β be a simple summation of the \mathcal{M} values. Our construction of the scheme was defined in the order of $O(2^{pT})$. It could be despairing at a glance, yet consider that in many languages without a list expression, $p \leq 5$ could be achieved, and T only increases with the density and size of the code chunk, which raw AST representation also suffers such a polynomial growth.

LEMMA 2. The polynomial-based CSBASG magnitude encoding is complete and optimal; there is no complete encoding with the maximum magnitude of the ASG matrix entry less than $O(2^{pT})$.

PROOF. Completeness follows since $1 \leq \omega \leq p$ always holds, for each integer $k \in \mathbb{Z}$ such that $\mathcal{M}(\omega, t) = 2^k$, there is a unique pair of ω and t , there is no Type 1 Confusion. Consider multiple AST links from the syntactically and semantically same parent node to the syntactically and semantically same child, each with $\omega_1, \omega_2, \dots, \omega_n$ as their positions, at t_1, t_2, \dots, t_n -th visit of the parent node. Then, $\sum_{j=1}^n 2^{(t_j-1)p+\omega_j} = \sum_{k=0}^{pT} \mathbb{I}\{\exists j = 1, \dots, n | k = (t_j - 1)p + \omega_j\} 2^k$ is a unique integer representation of the magnitude of an adjacency matrix entry in the ASG, so it is also free of Type 2 or Type 3 Confusion, gives the completeness of the representation. Optimality follows since each positive integer has a binary form $k = \sum_{j=0}^{\infty} c_j 2^j$,

$c_j \in \{0, 1\}$, which each $c_j = 1$ corresponds to an edge with $j = (t - 1)p + \omega$. \square

By Lemma 2, the summation-of-exponentials gives the most compact and accurate solution for the complete enumeration of the graph, and the creation of such a graph also depends on the enumerability of the grammar. However, a representation within the 32- or 64-bit bound could be achieved for less scaled language, such as Alloy. A heuristic generated by representation learning could also be achieved by learning the logarithmic parameters for a more generally purposed language with more syntactic elements and a larger AST.

The Decoding Algorithm

The decoding process is straightforward in theory. Words of the code are stored in correspondence to rows and columns of the matrix; each row or column corresponds to an individual word, and vice versa. Formally, we designate $L : \mathcal{G} \rightarrow \mathcal{T}$ as the parser that translates an ASG back to its uniquely corresponding AST. L is therefore a counterpart of Algorithm 1 and bounded by the constructions of \mathcal{M} and β functions. For each of the nonzero entries in the ASG adjacency matrix, we can break it into concrete links by reversing \mathcal{M} and β . For the binary polynomial-based magnitude encoding given above, we take the integer value of the magnitude $|a_{ij}|$ and break it with regard to its binary form: each digit signing 1 in the binary form corresponds to a concrete AST link. In this case, an ASG node was broken into a set of AST nodes, each with its corresponding outer edges by the visit order. Since the possible edges are all examined once and the size of the entries determines the binary forms, we have a complexity of $O(|\mathcal{E}| \log(\max(w_{i,j})))$ or $O(|\mathcal{V}|^2 \log(\max(w_{i,j})))$ for the decoding process.

4 APPLICATION OF CSBASG ON ALLOY

Alloy, a specification language, has plenty of features that construct a friendly scenario for CSBASG to apply. Firstly, as a first-order logic-based declarative language, we could easily construct a finite set of symbols given a model source code set. Besides, there are few infinitely extensible structures in its grammar, which limits the usage of empirical estimates of the maximum nodes under a given structure; furthermore, even the infinitely extensible structures could be assumed with a relatively low count of children. Its simplicity makes an ideal starting point for CSBASG representation.

To begin with, we utilize a parser that classifies the syntactic properties of the code keywords into a limited number of categories. After that, we need to set a p value corresponding to the maximum number of children for each category, for instance, 1 for unary operators, 2 for binary operators, 3 for if-then-else, and a more significant number for the several uncovered infinite categories. This could cause ambiguity in some edge cases. Still, since Alloy was used in modeling the structures within the scope of a category of sets, there will unlikely be any long enumerations over 10 or 15 items, so we use $p = 17$ for the categories without a precise, finite maximum children number. While completeness is not guaranteed, we are aiming at solving the absolute most of the cases; while it is possible to break the enumerations by putting the list of items into a linked structure, in most cases, the tradeoff of completeness

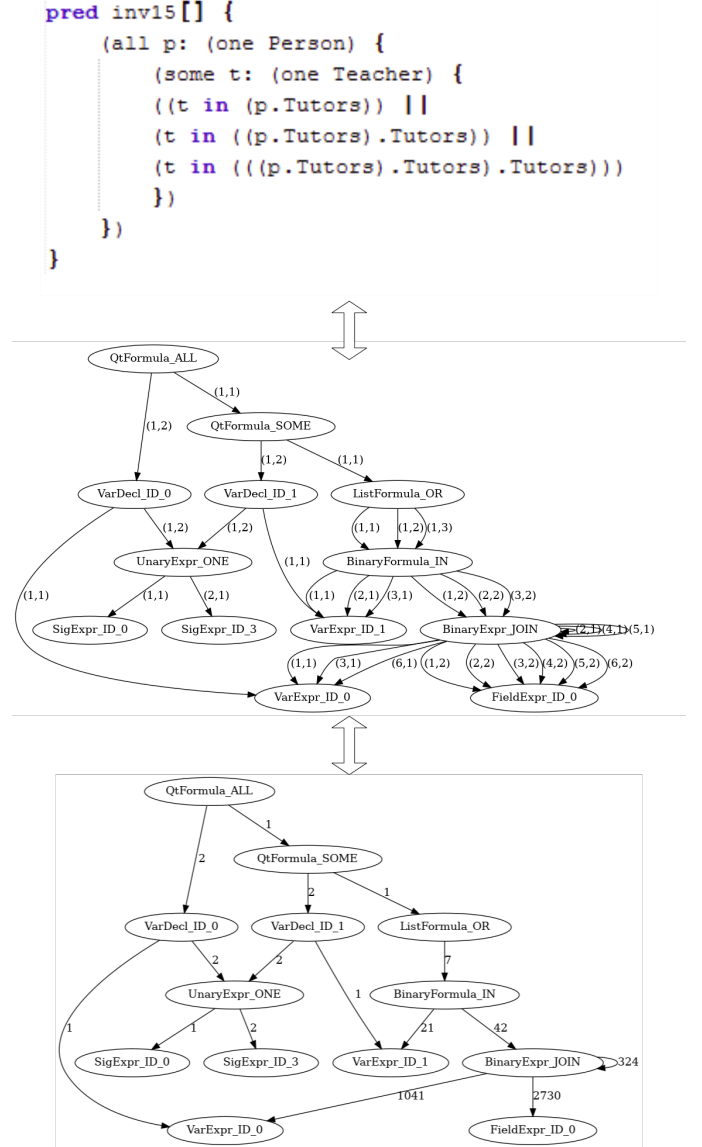


Figure 3: An example illustrating the compactness and simplicity of CSBASG; the original code (upper) could be expressed as an equivalent multigraph (middle) with the AST in Figure 1, and turns into the adjacency relationship (lower) with the polynomial-based encoding. With the same predicate in Figure 1, the number of nodes reduced significantly from 31 to 12. All edges are now assigned an integer weight value, which forms an adjacency matrix.

in the edge cases could deliver more benefits in intuitiveness and compactness of the representation.

Inside each category, the nodes are differentiated by their semantic contents, which are still finitely enumerable since we have access to the set signatures defined within a model file, and there are almost no numerical constants, so it is safe to assume that constants

are limited to booleans and small integers. In our approaches, we divided the AST nodes under a paragraph of an expression or formula into 19 categories, plus the zero-signature node signing the local root. Devolved from the syntactic categories are semantic subcategories, and the number of subcategories within a syntactic category ranges from 1 for the simple, invariant nodes to 32, which is the number of possible binary expressions.

Finally, we are required to assign the angular signatures for each node. In our practice, we used a simple encoding by dividing the interval of a circle $(-\pi, \pi)$ into equal-length intervals with $D = \pi/13$ as the length of each interval. For each interval, we assign subticks that divide it into 128 or 65536 sectors, depending on the syntactic category. By the scheme above, we have obtained each AST node’s syntactic-semantic pair (Ψ, ψ) using the results generated from the parser. Then, we map them on the unit circle as their signatures: each syntactic category goes with the beginning of a $\pi/13$ -length interval, and each subtick above the interval starting point corresponds to a semantic subcategory. Note that this is just a demonstration of encoding and is only defined for convenience but not learned for optimality, and the angular correspondence could be any bijective mappings.

Figure 3 gives an example of the encoding from an Alloy predicate AST to its corresponding CSBASG using a polynomial-based static scheme. The syntactic-semantic pairs in the table give the properties of each node in the AST and combine the AST nodes with identical semantic and syntactic properties. The angular signature assigned to each node is $\Psi D + \psi \delta$, where $\delta = D/128$ for expression or formula nodes and $\delta = D/65536$ for the relational declarations that would appear below a quantifying expression or formula, since by Alloy syntax multiple variables could be declared under the same relational declaration node. In our example, there are six JOIN binary operators (\cdot), which are represented as six distinct nodes in the original AST; in the ASG approach, the nodes are combined as a single node with the label BinaryExpr.JOIN.

The complex values could be used to compare two ASGs with shared parts, which will be discussed in Section 5.3.

5 EXPERIMENT

5.1 Dataset

Our dataset encompasses 6,307 models from Alloy4Fun[21], sourced from 8 different categories of problem, filtered from a larger dataset to ensure each is compliant, runnable, nonempty, and the student-written model is not completely identical with the ground truth. Each model has two predicates under a set of definitions of relations; a student writes one named *InvX* (or *PropX*, X is an identifying number) and is potentially faulty as a mutant predicate, and another called *InvXC* is the ground truth that gives a correct formula. Then we run two predicates, *overconstrained* and *underconstrained*, which determine if there are cases that satisfy *InvX* but not *InvXC*, or vice versa. If a model has no cases for both *overconstrained* and *underconstrained* predicates, then *InvX* is formally correct. This gives four categories of the models: correct ($InvX = InvXC$), overconstrained only ($InvX \subsetneq InvXC$), underconstrained ($InvXC \subsetneq InvX$), and both overconstrained and underconstrained ($InvX \not\subseteq InvXC \wedge InvXC \not\subseteq InvX$), covers all possible cases.

Dataset	#Models	Mut.Type	Mutant%	Correct%
lts	61	CORRECT	36.66	39.19
lts	113	UNDER	24.65	40.52
lts	138	BOTH	24.76	35.9
lts	66	UNDER	27.14	34.31
classroom_fol	495	CORRECT	32.83	14.67
classroom_fol	223	UNDER	30.48	16.86
classroom_fol	1115	BOTH	36.48	26.08
classroom_fol	166	UNDER	37.19	28.54
cv_v1	52	CORRECT	31.73	39.83
cv_v1	118	UNDER	36.05	41.48
cv_v1	68	BOTH	32.49	39.97
cv_v1	54	UNDER	32.03	37.94
train	75	CORRECT	29.44	19.43
train	170	UNDER	23.47	25.23
train	277	BOTH	28.18	28.54
train	174	UNDER	32.70	24.43
trash_rl	252	CORRECT	20.25	6.73
trash_rl	150	UNDER	13.42	7.10
trash_rl	267	BOTH	14.85	6.99
trash_rl	62	UNDER	31.67	11.68
cv_v2	31	CORRECT	30.95	40.47
cv_v2	40	UNDER	38.28	43.79
cv_v2	21	BOTH	38.37	43.08
cv_v2	12	UNDER	29.16	36.21
classroom_rl	495	CORRECT	32.83	14.67
classroom_rl	223	UNDER	30.48	16.86
classroom_rl	1115	BOTH	36.48	26.08
classroom_rl	166	UNDER	37.19	28.54
production	25	CORRECT	14.75	21.12
production	25	UNDER	18.84	20.73
production	22	BOTH	16.02	20.41
production	36	UNDER	22.89	22.80

Table 1: Compactness test results of the dataset. Each of the sub-dataset represents a category of problems within Alloy4Fun[21], and the student-written mutant predicates are categorized into four mutant types given their coverage of the set indicated by the ground truth: CORRECT, OVERconstrained, UNDERconstrained, or BOTH over- and underconstrained. The percentages given are the ratio of the reduction of nodes in the ASG representation compared to the raw AST.

5.2 Metric 1: Compactness of representation

We evaluate the compactness of the representation by the percentage of nodes in the ASG representation that are less than the raw AST. Overall, we achieved an impressive 27.25% reduction of nodes over the dataset, considering there is no loss of information, and the performance for each category of predicates is given in Table 1.

Note that since the dataset is mostly single predicates designed as after-class practices for college students, the probability of semantic identical nodes in the AST is relatively low, and for a sub-AST with a large scale, the performance would increase accordingly in the single-metric of node reduction. Moreover, the size of the adjacency

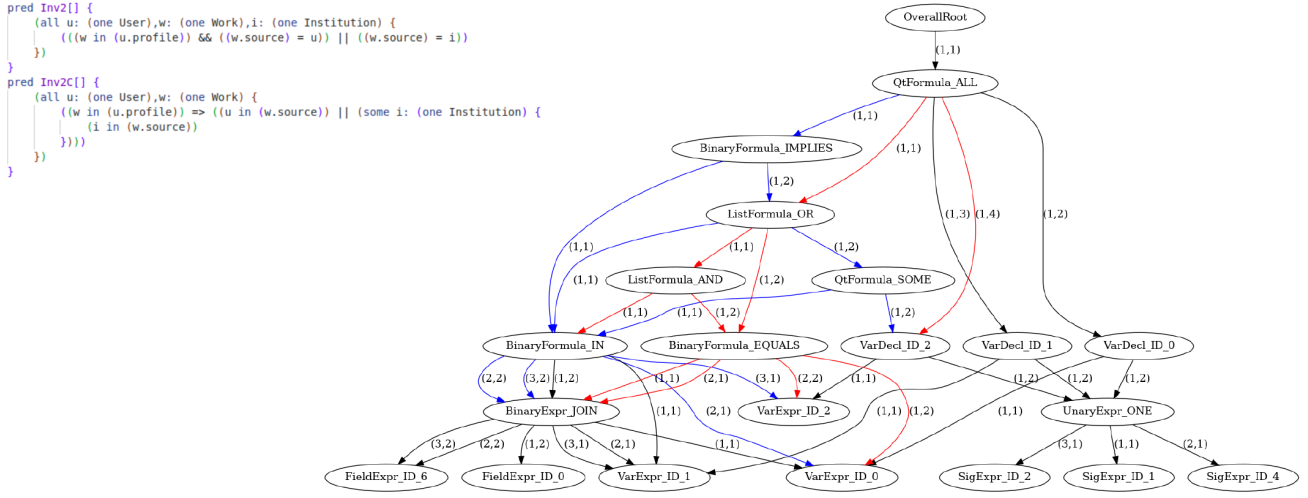


Figure 4: An example of a pair of student-written mutant predicate (Inv2) and the ground truth (Inv2C). The ASG edges in form (x, y) indicate the x -th visit of the sourcing node, and the positional relationship between the nodes is y . Black edges are present in both predicates, red edges are present in the mutant only, and blue edges are present in the ground truth only; a fixing process, in theory, removes all red edges and replaces them with blue ones.

matrix scales up with $O(N^2)$ with the number of nodes, so a denser matrix could be achieved with the ASG scheme.

However, this metric should not be confused with saving spaces. Since in an AST the entries in the adjacency matrix are either 0 (indicating no links) or 1 (indicating a direct link), which only occupy 1-bit per entry in an optimized language or computational method, but *Lemma 2* indicates that there is no complete encoding without information loss that takes a number smaller than $O(2^{pT})$ which occupies pT -bits at least, so space saving is neither guaranteed or indicated by the inference and experiment above.

5.3 Metric 2: A case study of comparability

Comparing a pair of code snippets to train a model for auto-correction could be tedious, especially for the syntactically correct faulty predicates. Comparability of the CSBASG could point out a direction of inquiry by the graph mutations. We have a simple formula to decode its multiedges, given our construction of the CSBASG with the polynomial method.

Since the dataset was written by students who have little experience in Alloy modeling and some of them write models that have few, if not zero, common edges; however, among them, there could also be some manual repairs that could be shown as a process of applying a set of “Atomic Mutations”. We call an atomic mutation either adding or removing an edge in the ASG; a relationship change between two nodes could also be represented as removing the old edge and adding the new one.

Figure 4 gives an example of the decoded CSBASG construction for comparing two predicates in the same declarative environment, the faulty and correct solution to the same problem. The common parts, as reflected by the subgraph characterized with black edges, show the correct declaration of the first two variables by the student

given the right part of the graph and the trivial correctness of the fields associated with the variables as elements of the pre-declared sets were shown in the bottom-left corner. However, most of the graph shows significant deviation of logic, as expected for the student-written mutant being both overconstrained and underconstrained. Straightforwardly, each of the red or blue edges in the graph is an atomic mutation between the pair of predicates; the red edge is a link to be broken, and the blue edge is a link to be established in a hypothetical automatic fixing application. In the example above, we could see that out of 41 edges shown in *Figure 4*, there are 10 common edges presenting in both the faulty model and the ground truth, 20 edges are added and 11 edges are removed from the faulty model, which are performs of atomic mutations.

To get a holistic review of the comparability by shared edges after decoding of the CSBASG, we use a simple metric by counting the percentage of the shared edges among the predicates, and the result is a significant evidence of comparability that shows 60.74% of edges in the corrected models also appearing in the student-written, possibly faulty mutant model; and 77.37% of edges in the faulty models also appears in its student-written counterpart. *Table 2* gives an illustration of per-category performance of comparability.

6 FUTURE WORKS

6.1 Laplacian of CSBASG and Mutant as a Control Operation

At the beginning of this research, we attempted to use the Laplacian matrix to represent the matrix. However, since some self-edges exist in the scope of the Alloy ASG, and a formally defined construction of a Laplacian matrix did not include this situation, a Laplacian construction for a directed graph containing self-edges is yet to

Dataset	#Models	Mut.Type	Mutant%	Correct%
lts	61	CORRECT	51.61	49.31
lts	113	UNDER	69.66	31.03
lts	138	BOTH	71.46	36.55
lts	66	UNDER	60.87	42.91
classroom_fol	495	CORRECT	82.07	71.77
classroom_fol	223	UNDER	77.54	63.51
classroom_fol	1115	BOTH	79.21	64.01
classroom_fol	166	UNDER	69.61	61.49
cv_v1	52	CORRECT	62.88	38.86
cv_v1	118	UNDER	58.99	34.84
cv_v1	68	BOTH	66.96	36.03
cv_v1	54	UNDER	69.96	37.52
train	75	CORRECT	66.66	63.86
train	170	UNDER	70.06	49.00
train	277	BOTH	75.16	50.97
train	174	UNDER	73.29	60.55
trash_rl	252	CORRECT	90.64	73.49
trash_rl	150	UNDER	84.08	61.93
trash_rl	267	BOTH	89.39	62.35
trash_rl	62	UNDER	90.21	75.24
cv_v2	31	CORRECT	63.93	38.38
cv_v2	40	UNDER	65.78	33.73
cv_v2	21	BOTH	67.67	35.04
cv_v2	12	UNDER	70.70	36.82
classroom_rl	495	CORRECT	82.07	71.77
classroom_rl	223	UNDER	77.54	63.51
classroom_rl	1115	BOTH	79.21	64.01
classroom_rl	166	UNDER	69.61	61.49
production	25	CORRECT	68.12	49.40
production	25	UNDER	71.80	45.60
production	22	BOTH	70.67	42.82
production	36	UNDER	43.86	45.62

Table 2: Comparability quantification results in the per-category experiment. The percentages given are the ratio of the edges that also presenting in its mutant or corrected counterpart with the same relationship (position and execution order), that is the percentage of the shared edges in each predicate.

be constructed. Nonetheless, technically, the CSBASG still holds its structural balance, and a direction of inquiry of mutants as control operations in a discrete-time system still holds. There are existing works [1, 26] suggesting constructions that could apply to various kinds of graphs with self-loops, which are potentially fitting constructions to apply for the application that regards a repairing process of a pair of code segments as a control system to develop further possible methods of a modification on a software system containing multiple functional code segments to be considered.

6.2 Learning of Encoding and Alloy Code Generation

In this paper, we only attempted to ensure a zero-information-loss encoding for Alloy code segments but still relied on the map of

nodes since we have a static, same-distance pre-defined encoding. Nevertheless, in theory, we can stop this reliance by ensuring no different pair of edges have the same angular signature difference.

Consider a vector $\zeta = [1\angle\theta_1, 1\angle\theta_2, \dots, 1\angle\theta_n]^T$ where n is the number of total nodes, such that, by *Lemma 1*, the eigenvector of the CSBASG. We could train this vector as an embedding of the nodes in the CSBASG, giving their angular signatures. In a future scenario, such a vector could be trained with some objective function in applications such as Alloy code generation. A common approach could be an optimization problem like

$$\min \sum_{i,j=1\dots n} \mathbb{I}((v_i, v_j) \in \mathcal{E})(\theta_i - \theta_j)$$

given $\theta_i \neq \theta_j$ for any $i \neq j$. For a sub-ASG containing solely expressions or formulae with such a vector ζ , we could estimate that it could be a high probability for an incomplete ASG to have edges connecting to the most possible nodes that have a lower angular signature distance with the parent node, helping us to fill out the blanks in an incomplete code segment or generate examples within a predefined declarative environment.

6.3 Automatic Fixing by Machine Learning

Our research was motivated by a requirement to take the programming logic into the machine learning models and create a toolset that could be utilized in automatic fixing. However, due to the limitation of our dataset, few models could be fixed by a small number of mutant operations. Nonetheless, since we already have a mechanism that could output the common edges, edges to be removed, and edges to be established, we could begin with a predictive model for the probability of the existence of each edge, as suggested by some classical graph neural networks, but adapting those methods on the directed multigraph with a polynomial encoding is still posing challenges to the future research.

7 CONCLUSION

This paper introduced a novel graph representation of the programming language as a complex-valued multigraph with a polynomial-based adjacency matrix encoding. It evaluated its applicability on the declarative specification language Alloy. It further evaluated its compactness improvement on a dataset consisting of multiple Alloy models and the comparability of the Alloy predicates in an attempt to develop an automatic fixing framework. It points out a direction of inquiry in utilizing the representation in multiple software engineering practices utilizing Alloy and possible integration in a machine learning algorithm.

REFERENCES

- [1] Behcet Acikmese. *Spectrum of Laplacians for Graphs with Self-Loops*. 2015. arXiv: 1505.08133 [math.OC].
- [2] Devdatta Akhawe et al. “Towards a Formal Foundation of Web Security”. In: *2010 23rd IEEE Computer Security Foundations Symposium*. 2010, pp. 290–304.
- [3] Abdulaziz Alhfeldhi et al. “Adversarial Patch Generation for Automatic Program Repair”. In: *ArXiv abs/2012.11060* (2020). URL: <https://api.semanticscholar.org/CorpusID:260510563>.

- [4] Uri Alon, Omer Levy, and Eran Yahav. “code2seq: Generating Sequences from Structured Representations of Code”. In: *International Conference on Learning Representations*. 2019. URL: <https://openreview.net/forum?id=H1gKY09tX>.
- [5] Hamid Bagheri et al. “A formal approach for detection of security flaws in the Android permission system”. In: *Formal Asp. Comput.* (2018).
- [6] I.D. Baxter et al. “Clone detection using abstract syntax trees”. In: *Proceedings. International Conference on Software Maintenance (Cat. No. 98CB36272)*. 1998, pp. 368–377. DOI: 10.1109/ICSM.1998.738528.
- [7] Jorge Cerqueira, Alcino Cunha, and Nuno Macedo. “Timely Specification Repair for Alloy 6”. In: *Software Engineering and Formal Methods: 20th International Conference, SEFM 2022, Berlin, Germany, September 26–30, 2022, Proceedings*. Berlin, Germany: Springer-Verlag, 2022, pp. 288–303. ISBN: 978-3-031-17107-9. DOI: 10.1007/978-3-031-17108-6_18. URL: https://doi.org/10.1007/978-3-031-17108-6_18.
- [8] Nathan Chong, Tyler Sorensen, and John Wickerson. “The Semantics of Transactions and Weak Memory in x86, Power, ARM, and C++”. In: *SIGPLAN Not.* 53.4 (2018), pp. 211–225.
- [9] Edward B. Duffy and Brian A. Malloy. “Design and Implementation of a Language-Complete C++ Semantic Graph”. In: *Proceedings of the 50th Annual Southeast Regional Conference. ACM-SE ’12*. Tuscaloosa, Alabama: Association for Computing Machinery, 2012, pp. 170–175. ISBN: 9781450312035. DOI: 10.1145/2184512.2184552. URL: <https://doi.org/10.1145/2184512.2184552>.
- [10] J. P. Galeotti et al. “TACO: Efficient SAT-Based Bounded Verification Using Symmetry Breaking and Tight Bounds”. In: *TSE* (2013).
- [11] Hongyang Gao, Zhengyang Wang, and Shuiwang Ji. “Large-Scale Learnable Graph Convolutional Networks”. In: *CoRR abs/1808.03965* (2018). arXiv: 1808.03965. URL: <http://arxiv.org/abs/1808.03965>.
- [12] Divya Gopinath, Muhammad Zubair Malik, and Sarfraz Khurshid. “Specification-Based Program Repair Using SAT”. In: *TACAS*. 2011, pp. 173–188.
- [13] Rahul Gupta et al. “DeepFix: Fixing Common C Language Errors by Deep Learning”. In: *Proceedings of the Thirty-First AAAI Conference on Artificial Intelligence*. AAAI’17. San Francisco, California, USA: AAAI Press, 2017, pp. 1345–1351.
- [14] Simón Gutiérrez Brida et al. “Bounded Exhaustive Search of Alloy Specification Repairs”. In: *2021 IEEE/ACM 43rd International Conference on Software Engineering (ICSE)*. 2021, pp. 1135–1147. DOI: 10.1109/ICSE43902.2021.00105.
- [15] Shan Huang, Xiao Zhou, and Sang Chin. “Application of Seq2Seq Models on Code Correction”. In: *Frontiers in Artificial Intelligence* 4 (2021). ISSN: 2624-8212. DOI: 10.3389/frai.2021.590215. URL: <https://www.frontiersin.org/articles/10.3389/frai.2021.590215>.
- [16] Daniel Jackson. “Alloy: A Lightweight Object Modelling Notation”. In: *ACM Trans. Softw. Eng. Methodol.* 11.2 (Apr. 2002), pp. 256–290. ISSN: 1049-331X. DOI: 10.1145/505145.505149. URL: <https://doi.org/10.1145/505145.505149>.
- [17] Daniel Jackson and Mandana Vaziri. “Finding Bugs with a Constraint Solver”. In: *ISSTA*. Aug. 2000.
- [18] Ruoyu Li et al. “Adaptive Graph Convolutional Neural Networks”. In: *Proceedings of the Thirty-Second AAAI Conference on Artificial Intelligence and Thirtieth Innovative Applications of Artificial Intelligence Conference and Eighth AAAI Symposium on Educational Advances in Artificial Intelligence*. AAAI’18/IAAI’18/EAAI’18. New Orleans, Louisiana, USA: AAAI Press, 2018. ISBN: 978-1-57735-800-8.
- [19] Fan Long, Peter Amidon, and Martin Rinard. “Automatic Inference of Code Transforms for Patch Generation”. In: *Proceedings of the 2017 11th Joint Meeting on Foundations of Software Engineering*. ESEC/FSE 2017. Paderborn, Germany: Association for Computing Machinery, 2017, pp. 727–739. ISBN: 9781450351058. DOI: 10.1145/3106237.3106253. URL: <https://doi.org/10.1145/3106237.3106253>.
- [20] Fan Long and Martin Rinard. “Automatic Patch Generation by Learning Correct Code”. In: *Proceedings of the 43rd Annual ACM SIGPLAN-SIGACT Symposium on Principles of Programming Languages*. POPL ’16. St. Petersburg, FL, USA: Association for Computing Machinery, 2016, pp. 298–312. ISBN: 9781450335492. DOI: 10.1145/2837614.2837617. URL: <https://doi.org/10.1145/2837614.2837617>.
- [21] Nuno Macedo et al. *Sharing and Learning Alloy on the Web*. 2019. arXiv: 1907.02275 [cs.CY].
- [22] Darko Marinov and Sarfraz Khurshid. “TestEra: A Novel Framework for Automated Testing of Java Programs”. In: *ASE*. 2001.
- [23] Timothy Nelson et al. “The Margrave Tool for Firewall Analysis”. In: *LISA*. 2010.
- [24] Mathias Niepert, Mohamed Ahmed, and Konstantin Kutzkov. “Learning Convolutional Neural Networks for Graphs”. In: *CoRR abs/1605.05273* (2016). arXiv: 1605.05273. URL: <http://arxiv.org/abs/1605.05273>.
- [25] Benjamin Paassen et al. “Mapping Python Programs to Vectors using Recursive Neural Encodings”. In: *Journal of Educational Data Mining* 13.3 (Oct. 2021). DOI: 10.5281/zenodo.5634224. URL: <https://doi.org/10.5281/zenodo.5634224>.
- [26] Ugasini Preetha P, M. Suresh, and Ebenezer Bonyah. “On the spectrum, energy and Laplacian energy of graphs with self-loops”. In: *Heliyon* 9.7 (2023), e17001. ISSN: 2405-8440. DOI: <https://doi.org/10.1016/j.heliyon.2023.e17001>. URL: <https://www.sciencedirect.com/science/article/pii/S2405844023042081>.
- [27] Michael Schlichtkrull et al. *Modeling Relational Data with Graph Convolutional Networks*. 2017. arXiv: 1703.06103 [stat.ML].
- [28] D. Sobania et al. “An Analysis of the Automatic Bug Fixing Performance of ChatGPT”. In: *2023 IEEE/ACM International Workshop on Automated Program Repair (APR)*. Los Alamitos, CA, USA: IEEE Computer Society, May 2023, pp. 23–30. DOI: 10.1109/APR59189.2023.00012. URL: <https://doi.ieeecomputersociety.org/10.1109/APR59189.2023.00012>.
- [29] Caroline Trippel, Daniel Lustig, and Margaret Martonosi. “Security Verification via Automatic Hardware-Aware Exploit Synthesis: The CheckMate Approach”. In: *IEEE Micro* (2019).
- [30] Michele Tufano et al. “An Empirical Study on Learning Bug-Fixing Patches in the Wild via Neural Machine Translation”. In: *ACM Trans. Softw. Eng. Methodol.* 28.4 (Sept. 2019). ISSN:

- 1049-331X. DOI: [10.1145/3340544](https://doi.org/10.1145/3340544). URL: <https://doi.org/10.1145/3340544>.
- [31] Hongwei Wang et al. *GraphGAN: Graph Representation Learning with Generative Adversarial Nets*. 2017. DOI: [10.48550/ARXIV.1711.08267](https://arxiv.org/abs/1711.08267). URL: <https://arxiv.org/abs/1711.08267>.
- [32] Kaiyuan Wang, Allison Sullivan, and Sarfraz Khurshid. “Automated Model Repair for Alloy”. In: *Proceedings of the 33rd ACM/IEEE International Conference on Automated Software Engineering*. ASE ’18. Montpellier, France: Association for Computing Machinery, 2018, pp. 577–588. ISBN: 9781450359375. DOI: [10.1145/3238147.3238162](https://doi.org/10.1145/3238147.3238162). URL: <https://doi.org/10.1145/3238147.3238162>.
- [33] Kesu Wang et al. “Unified Abstract Syntax Tree Representation Learning for Cross-Language Program Classification”. In: *Proceedings of the 30th IEEE/ACM International Conference on Program Comprehension*. ICPC ’22. Virtual Event: Association for Computing Machinery, 2022, pp. 390–400. ISBN: 9781450392983. DOI: [10.1145/3524610.3527915](https://doi.org/10.1145/3524610.3527915). URL: <https://doi.org/10.1145/3524610.3527915>.
- [34] John Wickerson et al. “Automatically Comparing Memory Consistency Models”. In: *POPL*. 2017.
- [35] Bingting Wu, Bin Liang, and Xiaofang Zhang. “Turn Tree into Graph: Automatic Code Review via Simplified AST Driven Graph Convolutional Network”. In: *Know.-Based Syst.* 252.C (Sept. 2022). ISSN: 0950-7051. DOI: [10.1016/j.knosys.2022.109450](https://doi.org/10.1016/j.knosys.2022.109450). URL: <https://doi.org/10.1016/j.knosys.2022.109450>.
- [36] Honghui Wu et al. “Structural Balance of Complex Weighted Graphs and Multi-Partite Consensus”. In: *IEEE Control Systems Letters* 7 (2023), pp. 3801–3806. DOI: [10.1109/LCSYS.2023.3341992](https://doi.org/10.1109/LCSYS.2023.3341992).
- [37] Honghui Wu et al. *Structural Balance of Complex Weighted Graphs and Multi-partite Consensus*. 2023. arXiv: [2311.04389](https://arxiv.org/abs/2311.04389) [eess.SY].
- [38] Geunseok Yang, Kyeongsic Min, and Byungjeong Lee. “Applying Deep Learning Algorithm to Automatic Bug Localization and Repair”. In: *Proceedings of the 35th Annual ACM Symposium on Applied Computing*. SAC ’20. Brno, Czech Republic: Association for Computing Machinery, 2020, pp. 1634–1641. ISBN: 9781450368667. DOI: [10.1145/3341105.3374005](https://doi.org/10.1145/3341105.3374005). URL: <https://doi.org/10.1145/3341105.3374005>.
- [39] Razieh Nokhbeh Zaeem and Sarfraz Khurshid. “Contract-Based Data Structure Repair Using Alloy”. In: *ECOOP*. 2010, pp. 577–598.
- [40] Pamela Zave. “How to Make Chord Correct (Using a Stable Base)”. In: *CoRR* abs/1502.06461 (2015).
- [41] Jian Zhang et al. “A Novel Neural Source Code Representation Based on Abstract Syntax Tree”. In: *2019 IEEE/ACM 41st International Conference on Software Engineering (ICSE)*. 2019, pp. 783–794. DOI: [10.1109/ICSE.2019.00086](https://doi.org/10.1109/ICSE.2019.00086).
- [42] Guolong Zheng et al. “ATR: Template-Based Repair for Alloy Specifications”. In: *Proceedings of the 31st ACM SIGSOFT International Symposium on Software Testing and Analysis*. ISSTA 2022. New York, NY, USA: Association for Computing Machinery, 2022, pp. 666–677. ISBN: 9781450393799. DOI: [10.1145/3533767.3534369](https://doi.org/10.1145/3533767.3534369). URL: <https://doi.org/10.1145/3533767.3534369>.